IMPEDANCE CONSIDERATIONS FOR THE APS UPGRADE*

R. R. Lindberg†, Argonne National Laboratory, Lemont, IL USA
A. Blednykh, Brookhaven National Laboratory, Upton, NY USA

Abstract

The APS-Upgrade is targeting a 42 pm lattice that requires strong magnets and small vacuum chambers. Hence, impedance is of significant concern. We overview recent progress on identifying and modeling vacuum components that are important sources of impedance in the ring, including photon absorbers, BPMs, and flange joints. We also show how these impact collective dynamics in the APS-U lattice.

IMPEDANCE MODELING

BPM-bellows Assembly

We need to ensure that the impedance associated with the BPM-bellows assembly is minimal, both to ensure a manageable impact to collective instabilities, and to minimize the levels of RF heating. Figure 1(a) shows a CAD-generated model of the BPM-bellows assembly. The GlidCop RF fingers are shown in light gray; each finger is tapered from 0.5 mm at the root to 0.3 mm at the tip and will be coated with 13 microns of silver. The central BPM housing is 12 mm from the beam and will be plated in Rhodium. A magnified GdfidL representation of a single BPM button is in Fig. 1(b). The BPM button is 8 mm in diameter and 2 mm thick, while the BPM pin dimensions have been tailored to best match the characteristic impedance to 50 Ohm (the minimum pin diameter is 0.65 mm).
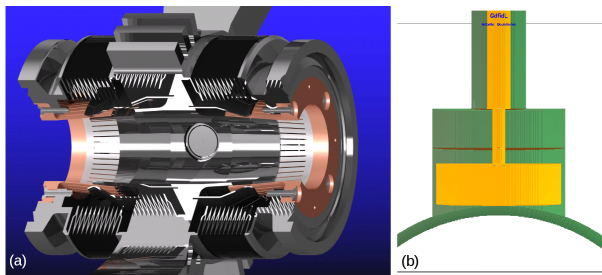
Figure 1: a) CAD model of the BPM-bellows assembly. b) GdfidL model of a single BPM button.

We used `GdfidL` [1] to compute the impedance of assembly; we plot the real and imaginary parts of the longitudinal $Z_\parallel$ in Fig. 2(a). The lowest resonance mode due to the button geometry is expected to have a frequency $f_{H11} \sim 11$ GHz, which we clearly see. This is well-beyond the bunch spectrum of the beam, so that we do not expect the beam to interact strongly with the bunch. Adding the real part $Z_\parallel$ to the contribution of the resistive wall, we then computed the

loss factor over a range of bunch lengths σ_z, from which we computed the expected RF heating shown in Fig. 2(b). In the case that the bunch-lengthening higher-harmonic cavity (HHC) is not functioning, we predict that $\sigma_z \approx 12$ mm and the power lost by the beam is sbout 2.8 W. If the HHC is tuned to flatten the potential we have $\sigma_z \approx 25$ mm and a power of 0.15 W, while if the HHC is set to maximize the lifetime by overstretching the bunch the loss is 0.05 W.
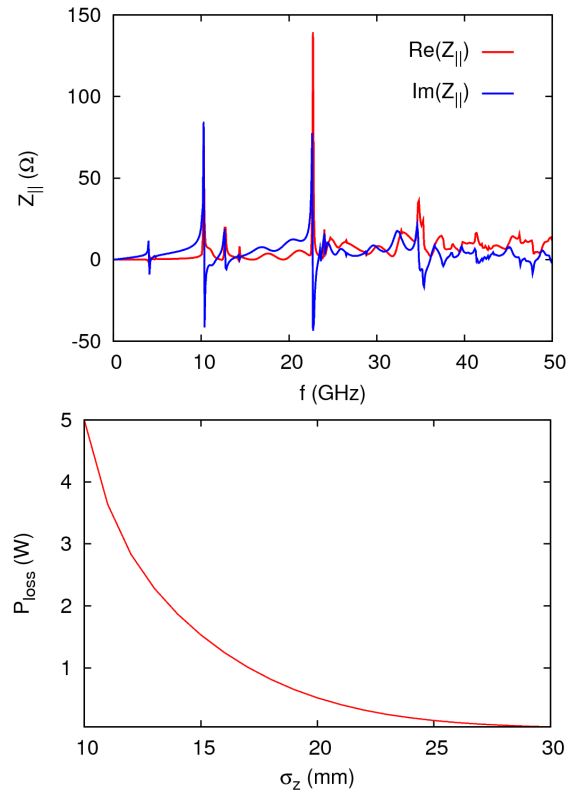
Figure 2: The real and imaginary parts of the BPM-bellows assembly impedance. Predicted RF heating level as a function of bunch length.

These levels of RF heating all appear to be manageable, but further simulations of precisely where the heat is deposited and how efficiently it can be transferred are planned. Finally, the assembly was just installed and removed for testing in the NSLS-II ring, and will be installed in the present APS for tests under beam.

In-line Photon Absorbers

What we call "in-line photon absorbers" are tapered restrictions whose purpose is to mask sensitive components from small to moderate levels of synchron radiation. Ray tracing simulations indicate that the absorbers must protrude into the chamber by typically 2–4 mm to provide the required

protection, and that 16 such absorbers are required in each sector. Because there are so many absorbers, they result in a large source of impedance within the ring that must be managed to the extent possible.
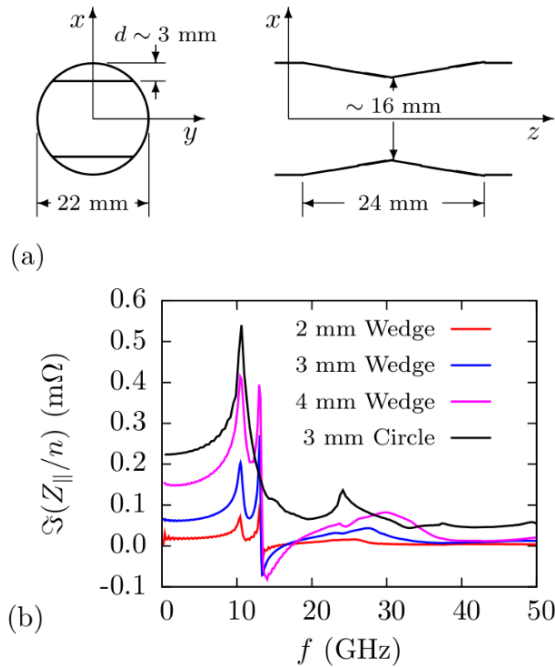
Figure 3: a) Geometry of the in-line photon absorber design. b) Comparison of the $\Im(Z_\parallel/n)$ for different protrusion depths d of the absorber. Black line shows the result for a cylindrically symmetric absorber for reference.

The basic design for the in-line absorbers was chosen to be a double wedge that is 24 mm long as shown in Fig. 3(a). This length allows for a small-angle taper to reduce the impedance, while still being short enough so that the absorber can be machined out of a flange. To minimize the impedance, the constriction only occurs in the horizontal plane, and is mirror symmetric in both planes to eliminate any on-axis transverse wakefields that might otherwise inflate the emittance. The resulting impedance is summarized by the $\Im(Z_\parallel/n)$ plotted in Fig. 3(b), where the impedance for three different absorber protrusion depths d are compared. The impedance is comparable to that of the bellows, and is less than half what it would be if the absorber were cylindrically symmetric.

RF Gaskets for Flanges

Flange gaps are another important potential source of impedance, primarily because the present vacumm design calls for 47 flanges per sector, for a total of 1880; the seemingly large number is because there are two for each BPM, while several others are required for the installation of several different chambers depending upon the magnet type. We have decided to use a gasket design the provides both a vacuum and RF seal, but at different locations. As shown in the top of Fig. 4, the gasket is essentially a large copper
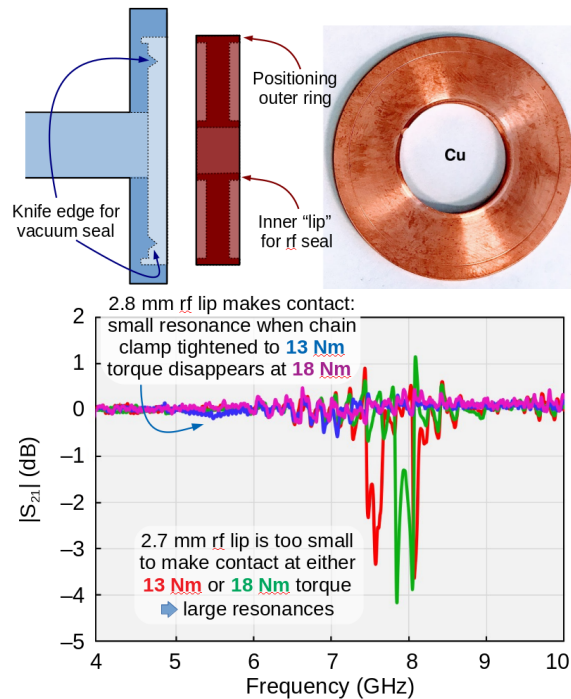
Figure 4: Top: Geometry of the RF gasket. Bottom: Transmission $|S_{21}|$ measurement of various gasket designs.

ring, whose outer surface is for the flange knife edge to make the vacuum seal, while having inner "RF lip" to provide RF contact at the 22 mm nominal diameter. The RF lip has small notches to allows conductance between the knife edge and the beam pipe, so there are no virtual leaks.

The height of the RF lip is an important design parameter: too short and there will be no RF contact; too tall and it will be tough to get a good vacuum seal. We tested for RF contact using the Goubau-line RF test stand [2], and show some results in bottom of Fig. 4. As one can see by the large resonant peaks, a 2.7 mm tall RF lip is too short, while the 2.8 mm height seems to be just tall enough. Interetesingly, for the 2.8 mm RF lip we saw a small, broad peak near 5.5 GHz when the clain clamp sealing the flange was torqued to 13 Nm, which went away when the torque was increased to 18 Nm.

LONGITUDINAL COLLECTIVE EFFECTS

From general considerations like that of the well-used Keil-Schell-Bousard criterion [3, 4], we expect that the microwave instability threshold to scale inversely with $Z_\parallel/n$. For this reason Table 1 lists the geometric ring summed $\Im(Z_\parallel/n)$ for all components presently in the impedance model, while Fig. 5(a) plots $\Im(Z_\parallel)$ for various combinations of components. The table shows that the BPM-bellows and in-line photon absorbers are the dominant drivers of the microwave instability, and that the contributions from the gate valves and flange gaps are also important. The latter of these is important merely because there are so many flanges in the ring.

Table 1: Summary of Longitudinal Impedance Contributions

Element	Number	$\sum \Im(Z_\parallel/n)$
BPM-bellows	560	0.051 Ω
Photon absorbers	640	0.048 Ω
Gate valves	160	0.015 Ω
Flange gaps	1880	0.011 Ω
Stripline kickers	8	0.009 Ω
Crotch Absorber	80	0.007 Ω
Other bellows	80	0.004 Ω
ID transitions	35	0.004 Ω
Pumping cross	200	0.002 Ω
TOTAL	NA	0.155 Ω

We are now in a position to use the impedance model described to assess various collective effects at the APS-U. Ref. [5] shows some results for transverse stability of the injected beam, and here we will focus on longitudinal collective effects in general and the microwave instability in particular. We do this using the particle tracking code `elegant` [6]; for these simulations we track 100,000 particles for 40,000 turns to determine the longitudinal equilibrium as a function of current. The transverse coordinates are tracked using the fast `ILMATRIX` element, which advances the coordinates using the tunes, beta-functions, and their dependence upon energy (chromaticity) and amplitude. We include both the synchrotron radiation and the longitudinal impedance as lumped elements, using the `SREFFECTS` and `ZLONGIT` element, respectively.

For the first set of simulations we treat both the main and bunch-lengthening higher-harmonic cavity (HHC) as active systems that are tuned to produce a quartic potential. We show predictions of the resulting bunch lengthening and energy spread increase in Fig. 5. Panel (b) shows that the bunch length increases significantly as the single-bunch current is raised to the 4.2 mA required for 48-bunch mode. Furthermore, Fig. 5(c) indicates an increase in σ_δ and the onset of the microwave instability at about 2.5 mA which is 4 times the 0.62 mA used in 324 bunch mode. This implies 48-bunch mode will be microave unstable, and that the longitudinal parameters may suffer fluctuations as indicated by the error bars in Fig. 5(b)-(c).

It turns out that the energy spread increase predicted by Fig. 5(c) is overly pessimistic. This is because the APS-U HHC will be a passive cavity tuned to maximize the lifetime, which turns out to lead to an overstretching configuration that further reduces the peak current. To determine what implication this has on the microwave instability, we varied the number of bunches assuming 200 mA average current. These simulations modeled the RF cavities as `RFMODE` elements that fully include beam loading, with the main cavities being externally driven and the harmonic cavities tuned to stretch the bunch to ~ 100 ps which maximizes lifetime. We plot the predicted energy spread as a function of the number of bunches in Fig. 6(a), which shows that overstretching
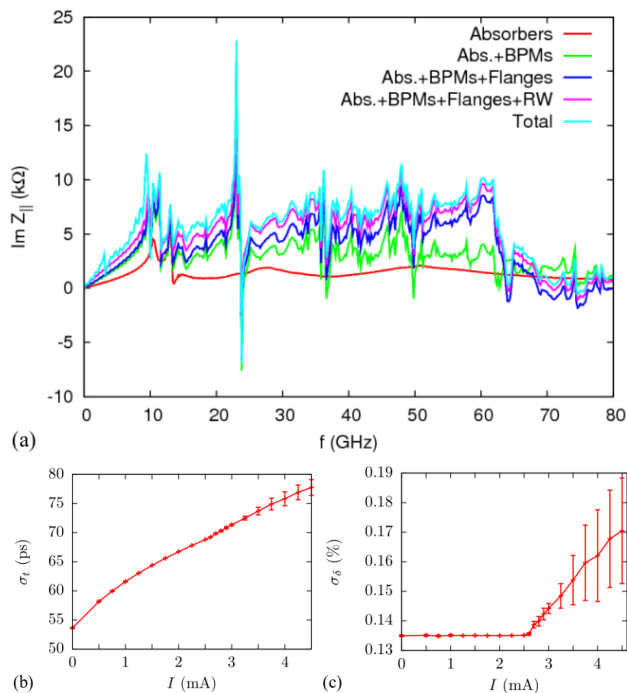
Figure 5: (a) Breakdown of $\Im(Z_\parallel)$ for the APS-U ring. Predicted bunch lengthening (a) and energy spread increase (b) for HHC tuned to produce quartic potential. The error bars indicate flucuations.

the bunch significantly increases the microwave instability threshold and that now 48-bunch mode is only just above the microwave instability threshold. In this case the longitudinal fluctuations are also significantly reduced, and the phase space portrait in Fig. 6(b) only shows a little evidence of the disturbance due to the instability.
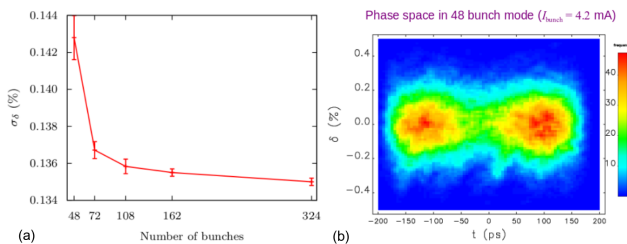
Figure 6: (a) Equilibrium energy spread as a function of bunch pattern for the self-consistent HHC set to overstretch the bunch. (b) Longitudinal phase space in 48-bunch mode.

CONCLUSIONS

We have shown some of the impedance analysis that has gone into the design of various vacuum components for the APS-U. Results so far have shown that the impedance is under control and with small leveles of RF heating over a range of longitudinal parameters. In particular, we have shown that the microwave instability minimally impacts the overstretched bunches planned for the APS-U.

REFERENCES

[1] W. Bruns, *The GdfidL Electromagnetic Field simulator*, `http://www.gdfidl.de`

[2] M. P. Sangroula, R. M. Lill, R. R. Lindberg, and R. B. Zabel, "Measuring the Coupling Impedance of Vacuum Components for the Advanced Photon Source Upgrade Using a Goubau Line", in *Proc. 9th Int. Particle Accelerator Conf. (IPAC'18)*, Vancouver, Canada, Apr.-May 2018, pp. 3211–3214. `doi:10.18429/JACoW-IPAC2018-THPAK005`

[3] E. Keil and W. Schnell, "Concerning longitudinal stability in the ISR," CERN/SPS Rep. ISR/TH/RF/69-48, 1969.

[4] D. Boussard, "Observation of microwave longitudinal instabilities in the CPS," CERN Rep. LabII/RF/INT/75-2, 1975.

[5] R. R. Lindberg, "Controlling Transient Collective Instabilities During Swap-Out Injection," presented at the North American Particle Accelerator Conf. (NAPAC'19), Lansing, MI, USA, Aug.-Sep. 2019, paper MOPLM08, this conference.

[6] M. Borland, "`elegant`: A Flexible SDDS-Compliant Code for Accelerator Simulation," ANL/APS LS-287, 2000.